SUPPLEMENTARY INFORMATION

Brain-based Predictions of Psychiatric Illness-Linked Behaviors Across the Sexes

Dhamala *et al.*

Supplemental Methods

Sample Construction

The ABCD dataset is a large community-based sample of children and adolescents who were assessed on a comprehensive set of neuroimaging, behavioral, developmental, and psychiatric batteries. This study used minimally preprocessed data from the Adolescent Brain Cognitive Development (ABCD). Specifically, data were obtained from the NIMH Data Archive for ABCD Release 2.0.1. The ABCD 2.0.1 Data Release included a total of 11,875 participants. MR images were acquired across 21 sites in the United States using harmonized protocols for GE and Siemens scanners. In line with our prior work(1, 2), exclusion criteria were used to ensure quality control. As recommended by the ABCD consortium, we excluded individuals who were scanned using Philips scanners due to incorrect preprocessing (https://github.com/ABCD-STUDY/fMRI-cleanup). For the T1 data, individuals who did not pass recon-all quality control(3) were removed. For the functional connectivity data, functional runs with boundary-based registration (BBR) costs greater than 0.6 were excluded. Further, volumes with framewise displacement (FD) > 0.3 mm or voxel-wise differentiated signal variance (DVARS) > 50, along with one volume before and two volumes after, were marked as outliers and subsequently censored. Uncensored segments of data containing fewer than five contiguous volumes were also censored(4, 5). Functional runs with over half of their volumes censored and/or max FD > 5mm were removed. Individuals who did not have at least 4 minutes of data were also excluded from further analysis. Individuals who did not have all behavioral measures were also excluded. Finally, we excluded siblings to prevent unintended biases due to inherent heritability in neurobiological and/or behavioral measures. Our final sample included comprised 5260 children (2689 males, 2571 females; 9-10 years old).

Behavioral Data

The Child Behavior Checklist is a widely used clinical scale for identifying problematic behaviors in children and adolescents(6), and includes eight empirically-based syndrome scales: Anxious/Depressed, Withdrawn/Depressed, Somatic Complaints, Social Problems, Thought Problems, Attention Problems Rule-Breaking Behavior, and Aggressive Behavior. These scores are further summarized into Internalizing, Externalizing, and Total Problems. The Internalizing domain summarizes Anxious/Depressed, Withdrawn/Depressed, and Somatic Complaints. The Externalizing domains summarizes Rule-Breaking and Aggressive Behaviors. Finally, the Total Problems score is based on responses to all of the eight syndrome scales. The CBCL also includes six Diagnostic and Statistical Manual of Mental Disorders (DSM)-oriented scales consistent with DSM-5 categories: Affective (Depressive), Anxiety, Somatic, Oppositional Defiant, Conduct, and Attention Deficit/Hyperactivity (ADHD) Disorders.

Preprocessing

Minimally preprocessed T1 data were further processed using FreeSurfer 5.3.0(7-10) to generate cortical surface meshes for each individual, which were then registered to a common spherical coordinate system(9, 10). Minimally preprocessed fMRI data were further processed with the following steps: (1) removal of initial frames, with the number of frames removed depending on the type of scanner(3) and (2) alignment with the T1 images using boundary-based registration(11) with FsFast. Framewise displacement (FD)(12) and voxel-wise differentiated signal variance (DVARS)(13) were computed using fsl_motion_outliers. Respiratory pseudomotion was filtered out using a bandstop filter (0.31-0.43 Hz) before computing FD(14-16). A total of 18 nuisance covariates were also regressed out of the fMRI time series: global signal, six motion correction parameters, averaged ventricular signal, averaged white matter signal, and their temporal derivatives. Regression coefficients were estimated from the non-censored volumes. Global signal regression was performance as we are

interested in behavioral prediction, and global signal regression has been shown to improve behavioral prediction performance(17, 18). Finally, the brain scans were interpolated across censored frames using least squares spectral estimation(19), band-pass filtered (0.009 Hz ≤ f ≤ 0.08 Hz), projected onto FreeSurfer fsaverage6 surface space, and smoothed using a 6 mm full-width half maximum kernel. All processing as described was completed on a local server.

Predictive Modeling

For each sex, we split the data into 100 distinct train and test sets (at approximately a 2:1 ratio) without replacement. Imaging site was considered when splitting the data such that we placed all participants from a given site either in the train or test set but not split across the two. Within each train set, we optimized the regularization parameter using three-fold cross-validation while similarly accounting for imaging site as in the initial train-test split. Once optimized, we evaluated models on the corresponding test set. We repeated this process for each of 100 distinct train-test splits to obtain a distribution of prediction accuracy. To evaluate model significance, for each set of predictive models, a corresponding set of null models was generated as follows: the behavioral score was randomly permuted 1000 times, and each permutation was used to train and test a null model using a randomly selected regularization parameter from the set of selected parameters from the original model. Prediction accuracy from each of the null models was then compared to the average accuracy from the corresponding distribution of model accuracies and model generalizabilities from the original (true) models. The p-value for each model's significance is defined as the proportion of null models with prediction accuracies greater than or equal to corresponding average accuracy from the original (true) distribution. All p-values were corrected for multiple comparisons across all measures of model accuracy and generalizability (i.e., 17 train behaviors x 2 train sexes x 17 test behaviors x 2 test sexes = 1156 comparisons) using the Benjamini-Hochberg False Discovery Rate (q=0.05) procedure(20).

Feature Weights

We used the Haufe transformation(21) to transform feature weights obtained from the linear ridge regression models to increase their interpretability and reliability(2, 22, 23). For each train split, we used feature weights obtained from the model, W, the covariance of the input data (functional connectivity), Σ_x, and the covariance of the output data (behavioral score), Σ_y, to compute the Haufe-transformed feature weights, A, as follows:

$$A = \Sigma_x W \Sigma_y^{-1}$$

We then averaged these Haufe-transformed feature weights across the 100 splits to obtain a mean feature importance value. We computed full correlations between mean feature importance obtained from the different models to evaluate whether they relied on shared or unique features to predict the behavioral scores. For all models, we also summarized pairwise regional feature importance at a network-level to support interpretability as previously described(24). Briefly, cortical parcels were assigned to one of 17 networks from the Yeo 17-network parcellation(25), and subcortical, brainstem, and cerebellar parcels were assigned to a single subcortical network for convenience. Regional pairwise positive and negative feature weights were separately averaged to yield network-level estimates of positive and negative associations between functional connectivity and behavioral scores.

Supplementary Table 1: Demographic information.
Demographic information (age, race/ethnicity, and socioeconomic status/income) for all subjects from the ABCD 2.0.1 Data Release. Demographic information are reported separately for subjects who are included (n=5260) and excluded (n=6615) from these analyses based on the criteria described in the Supplemental Methods. Data are further reported separately for males and females in both the included and excluded criteria. Reported proportions (%) may not sum to exactly 100% due to rounding.

Demographics	**Included (n=5260)**		**Excluded (n=6615)**	
	Males (n=2689)	**Females (n=2571)**	**Males (n=3499)**	**Females (3110)**
Age (months; mean ± standard deviation)	119.5 ± 7.5	119.1 ± 7.5	118.9 ± 7.4	118.5 ± 7.4
Race/Ethnicity (count, proportion)				
Asian	49, 1.8%	66, 2.6%	72, 2.1%	64, 2.1%
Black	355, 13.2%	362, 14.1%	532, 15.2%	530, 17.0%
Hispanic	535, 19.9%	555, 21.6%	714, 20.4%	602, 19.4%
Other	267, 9.9%	281, 10.9%	379, 10.8%	317, 10.2%
White	1479, 55.0%	1304, 50.7%	1796, 51.3%	1595, 51.3%
No Response	4, 0.1%	3, 0.1%	6, 0.2%	2, 0.1%
Socioeconomic Status/Income (count, proportion)				
< $,5000	90, 3.3%	67, 2.6%	129, 3.7%	130, 4.2%
$5,000 – 11,999	89, 3.3%	83, 3.2%	122, 3.5%	128, 4.1%
$12,000 – 15,999	52, 1.9%	53, 2.1%	88, 2.5%	80, 2.6%
$16,000 – 24,999	106, 3.9%	105, 4.1%	181, 5.2%	130, 4.2%
$25,000 – 34,999	135, 5.0%	165, 6.4%	178, 5.1%	175, 5.6%
$35,000 – 49,999	209, 7.8%	202, 7.9%	269, 7.7%	254, 8.2%
$50,000 – 74,999	350, 13.0%	309, 12.0%	448, 12.8%	392, 12.6%
$75,000 – 99,999	376, 14.0%	368, 14.3%	428, 12.2%	399, 12.8%
$100,000 – 199,999	767, 28.5%	722, 28.1%	979, 28.0%	847, 27.2%
> $200,000	289, 10.7%	297, 11.6%	358, 10.2%	305, 9.8%
Don't know	116, 4.3%	97, 3.8%	151, 3.5%	140, 4.5%
Refuse to Answer	110, 4.1%	103, 4.0%	168, 4.8%	130, 4.2%

Supplementary Table 2: Males and females exhibit largely overlapping behavioral scores. Mean, median, standard deviation (SD), interquartile range (IQR), and corrected p values (*p*) corresponding to significant sex differences in behavioral scores. Sex differences with corrected p values < 0.01 were considered statistically significant. Behaviors with significant sex differences are bolded.

Behavior	**Males**				**Females**				***p***
	Mean	**Median**	**SD**	**IQR**	**Mean**	**Median**	**SD**	**IQR**	
Internalizing	5.2	3.0	5.7	6.0	5.3	4.0	5.6	6.0	0.077
Anxious/Depressed	2.6	1.0	3.2	4.0	2.7	2.0	3.1	4.0	0.045
Withdrawn/Depressed	1.1	0.0	1.8	2.0	1.0	0.0	1.6	1.0	**0.006**
Somatic Complaints	1.5	1.0	1.9	2.0	1.7	1.0	2.0	3.0	**0.000**
Externalizing	5.0	3.0	6.3	6.0	3.9	2.0	5.1	6.0	**0.000**
Rule-Breaking Behavior	1.4	1.0	2.0	2.0	0.9	0.0	1.6	1.0	**0.000**
Aggressive Behavior	3.6	2.0	4.7	5.0	2.9	2.0	3.9	4.0	**0.000**
Thought Problems	1.8	1.0	2.3	3.0	1.5	1.0	2.0	2.0	**0.000**
Attention Problems	3.4	2.0	3.7	5.0	2.5	1.0	3.1	4.0	**0.000**
Social Problems	1.7	1.0	2.4	2.0	1.6	1.0	2.2	2.0	0.106
Total Problems	19.8	14.0	19.0	21.0	16.9	12.0	16.5	19.0	**0.000**
Affective	1.4	1.0	2.1	2.0	1.2	0.0	1.9	2.0	**0.000**
Anxiety	2.1	1.0	2.5	3.0	2.2	1.0	2.5	3.0	0.026
Somatic	1.0	0.0	1.5	2.0	1.2	1.0	1.6	2.0	**0.000**
Oppositional Defiant	2.0	1.0	2.2	3.0	1.6	1.0	1.9	3.0	**0.000**
Conduct	1.5	0.0	2.6	2.0	1.0	0.0	1.9	1.0	**0.000**
ADHD	3.0	2.0	3.1	5.0	2.2	1.0	2.7	4.0	**0.000**

Supplementary Table 3: Motion is not related to psychopathological behavior.
Correlation coefficient between mean framewise displacement (FD) and behavioral scores for males and females.

Behavior	Males	Females
Internalizing	0.00	0.02
Anxious/Depressed	0.01	0.03
Withdrawn/Depressed	-0.01	0.01
Somatic Complaints	0.00	0.00
Externalizing	-0.03	0.03
Rule-Breaking Behavior	-0.03	0.03
Aggressive Behavior	-0.02	0.03
Thought Problems	-0.01	0.02
Attention Problems	-0.01	0.01
Social Problems	-0.01	0.02
Total Problems	-0.01	0.02
Affective	0.00	0.00
Anxiety	0.01	0.04
Somatic	0.00	0.00
Oppositional Defiant	-0.01	0.02
Conduct	-0.03	0.02
ADHD	-0.01	0.02

Supplementary Table 4: Shared network-level features underlie psychiatric illness-linked behaviors across the sexes.
Correlation coefficient between network-level feature weights from models trained on males and females. Correlations were computed separately for positive associations and negative associations. Corresponding network-level positive and negative associations for all behaviors for males and females are shown in Figures 5-7 and Supplementary Figures 1-14.

Behavior	Positive Associations	Negative Associations
Internalizing	0.66	0.72
Anxious/Depressed	0.55	0.73
Withdrawn/Depressed	0.89	0.72
Somatic Complaints	0.78	0.54
Externalizing	0.87	0.89
Rule-Breaking Behavior	0.90	0.94
Aggressive Behavior	0.80	0.75
Thought Problems	0.91	0.86
Attention Problems	0.95	0.94
Social Problems	0.82	0.90
Total Problems	0.95	0.88
Affective	0.81	0.75
Anxiety	0.38	0.53
Somatic	0.76	0.56
Oppositional Defiant	0.50	0.27
Conduct	0.89	0.93
ADHD	0.91	0.94

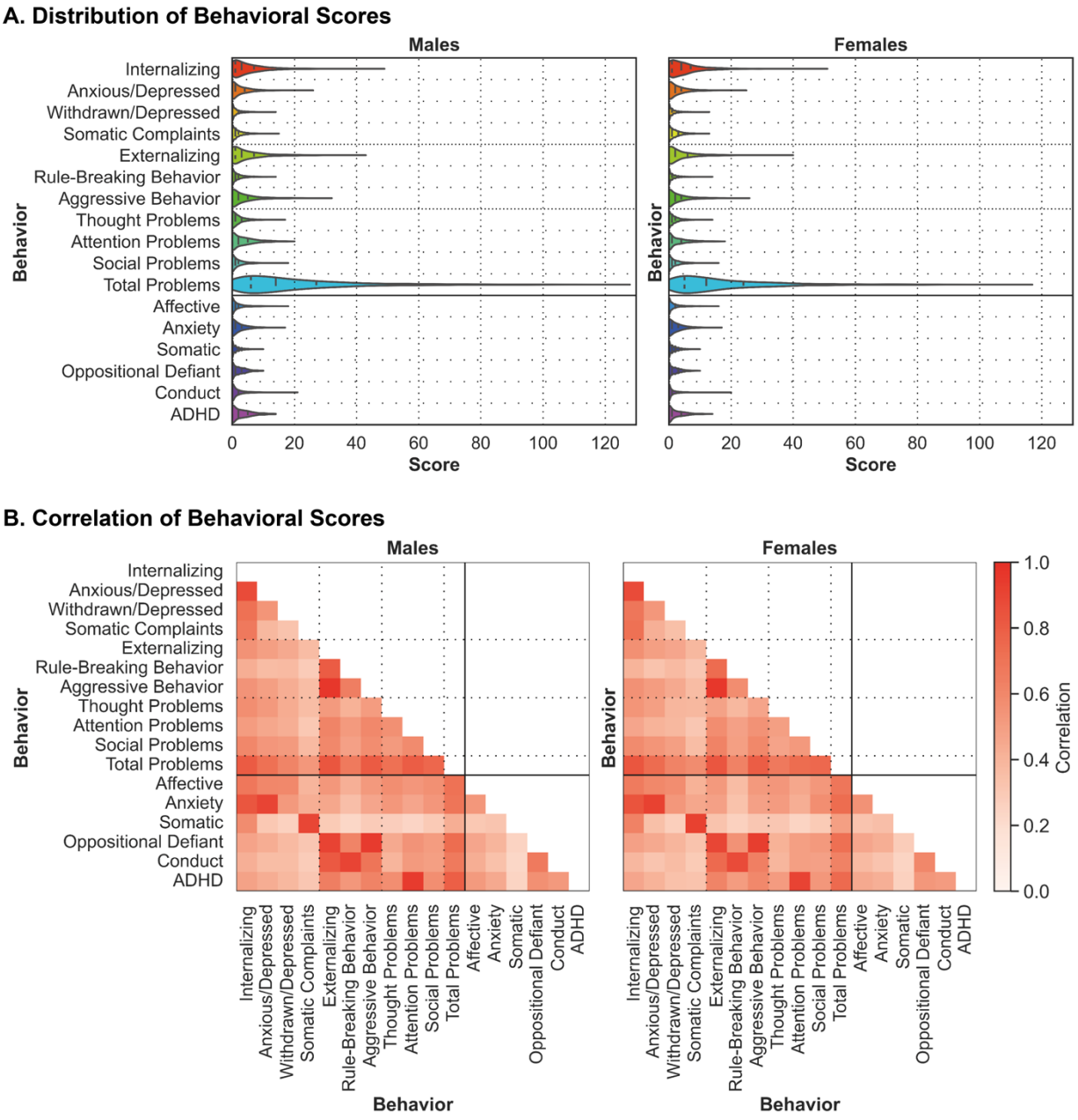

Supplementary Figure 1: Males and females exhibit similar behavioral trends.
(A) Violin plots display the distribution of all behavioral scores for males (left) and females (right). The shape of the violin plots indicates the entire distribution of values, dashed lines indicate the median, and dotted lines indicate the interquartile range. (B) The 2D grids display the correlation coefficient for each pair of behavioral scores for males (left) and females (right). ADHD – Attention deficit/hyperactivity disorder.

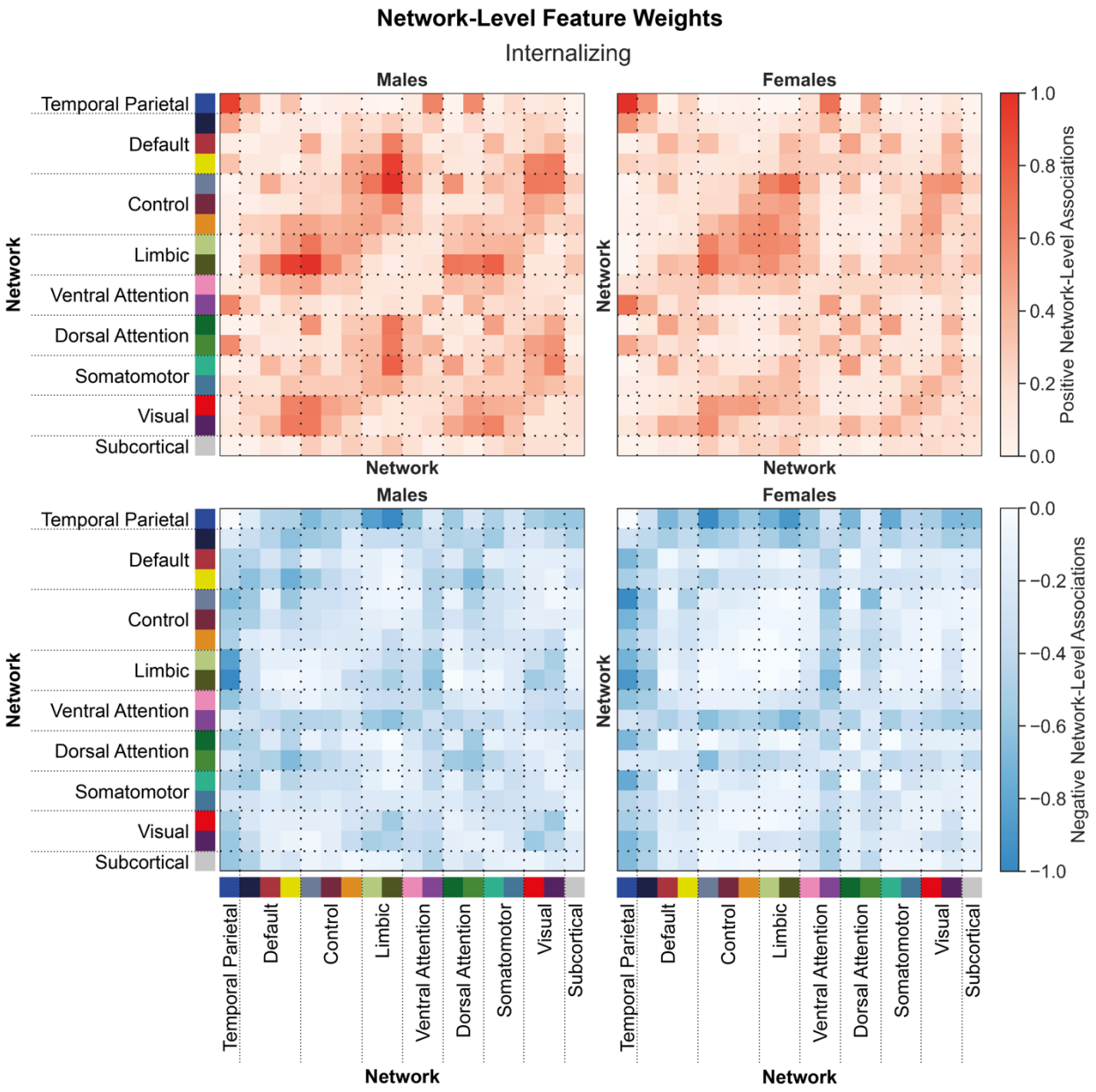

Supplementary Figure 2: Shared network-level functional connections underlying internalizing behaviors in males and females.
Positive (top) and negative (bottom) associations between network-level functional connectivity and internalizing behaviors in males (left) and females (right). Regional feature weights were summarized to a network-level by assigning cortical regions to one of 17 Yeo networks, and subcortical regions to a subcortical network. Colors next to the network labels along the vertical and horizontal axes correspond to the network colors from Figure 1C. Warmer colors within the heatmap indicate a positive association and cooler colors indicate a negative association. For visualization, values within each matrix were divided by the absolute maximum value across the positive and negative matrices for each sex. Correlations between positive associations across sexes, $r_{positive}$=0.66. Correlations between negative associations across sexes, $r_{negative}$=0.72.

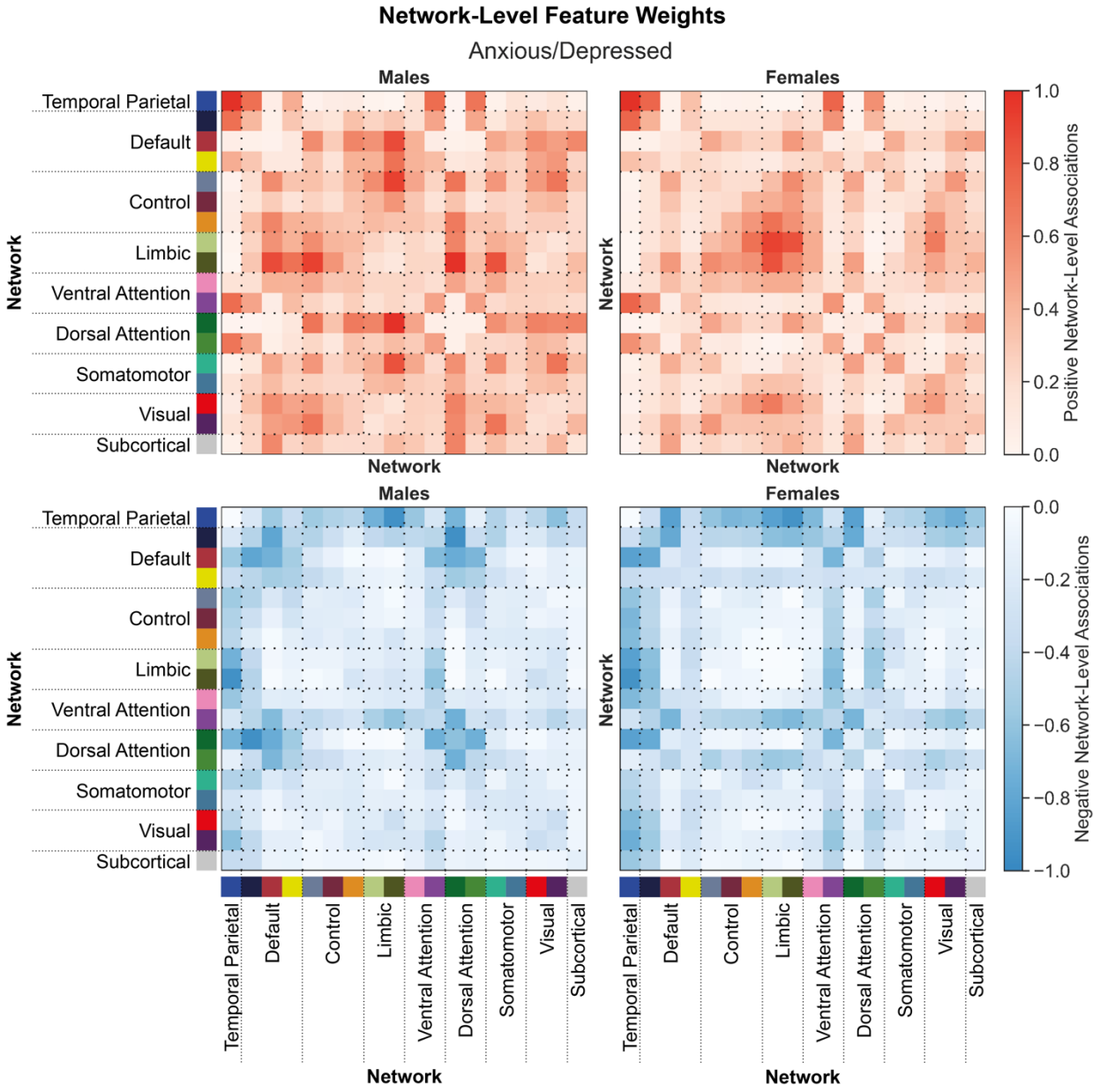

Supplementary Figure 3: Shared network-level functional connections underlying anxious/depressed behaviors in males and females.
Positive (top) and negative (bottom) associations between network-level functional connectivity and anxious/depressed behaviors in males (left) and females (right). Regional feature weights were summarized to a network-level by assigning cortical regions to one of 17 Yeo networks, and subcortical regions to a subcortical network. Colors next to the network labels along the vertical and horizontal axes correspond to the network colors from Figure 1C. Warmer colors within the heatmap indicate a positive association and cooler colors indicate a negative association. For visualization, values within each matrix were divided by the absolute maximum value across the positive and negative matrices for each sex. Correlations between positive associations across sexes, $r_{positive}$=0.55. Correlations between negative associations across sexes, $r_{negative}$=0.73.

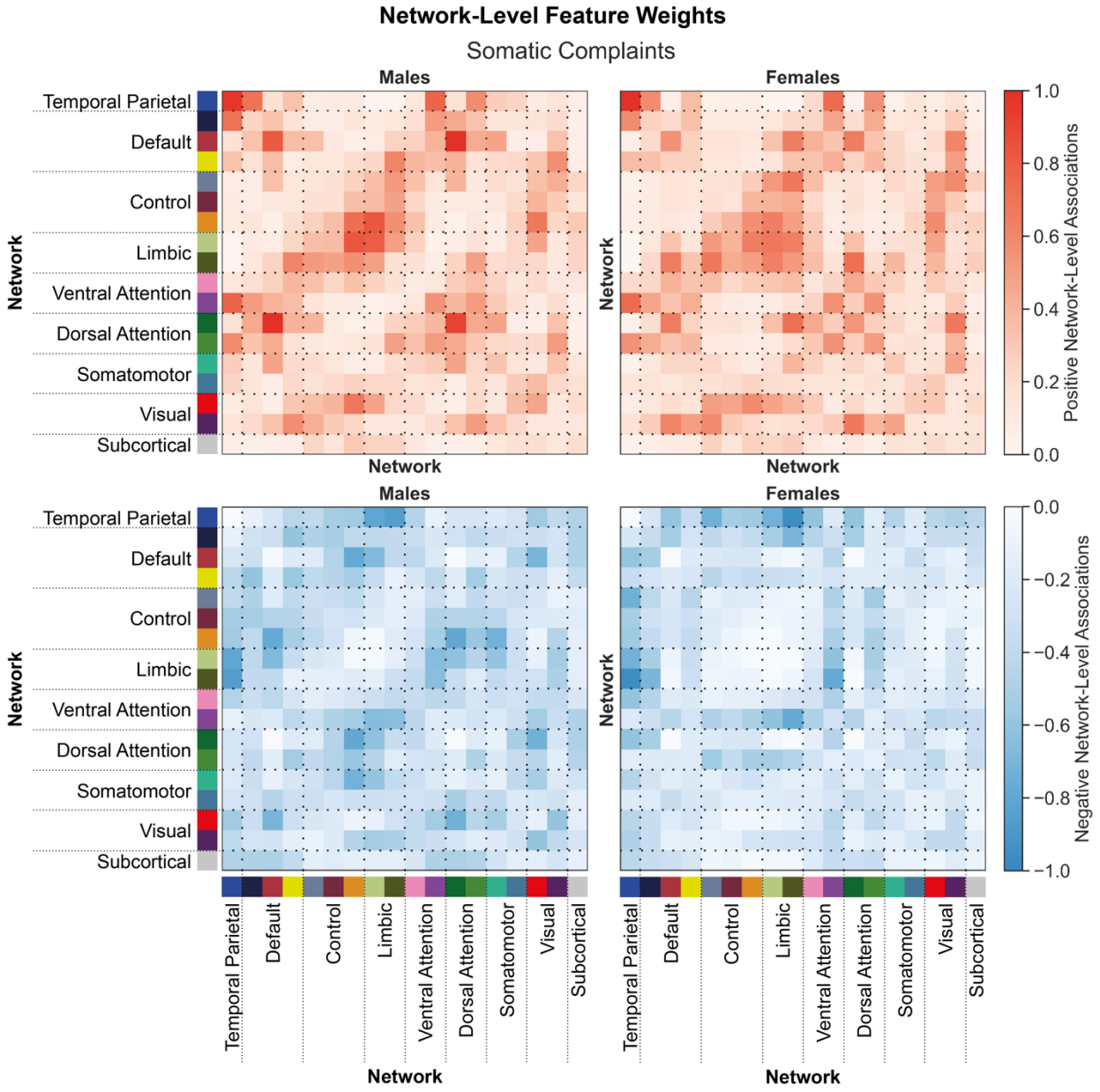

Supplementary Figure 4: Shared network-level functional connections underlying somatic complaints in males and females.
Positive (top) and negative (bottom) associations between network-level functional connectivity and somatic complaints in males (left) and females (right). Regional feature weights were summarized to a network-level by assigning cortical regions to one of 17 Yeo networks, and subcortical regions to a subcortical network. Colors next to the network labels along the vertical and horizontal axes correspond to the network colors from Figure 1C. Warmer colors within the heatmap indicate a positive association and cooler colors indicate a negative association. For visualization, values within each matrix were divided by the absolute maximum value across the positive and negative matrices for each sex. Correlations between positive associations across sexes, $r_{positive}$=0.78. Correlations between negative associations across sexes, $r_{negative}$=0.54.

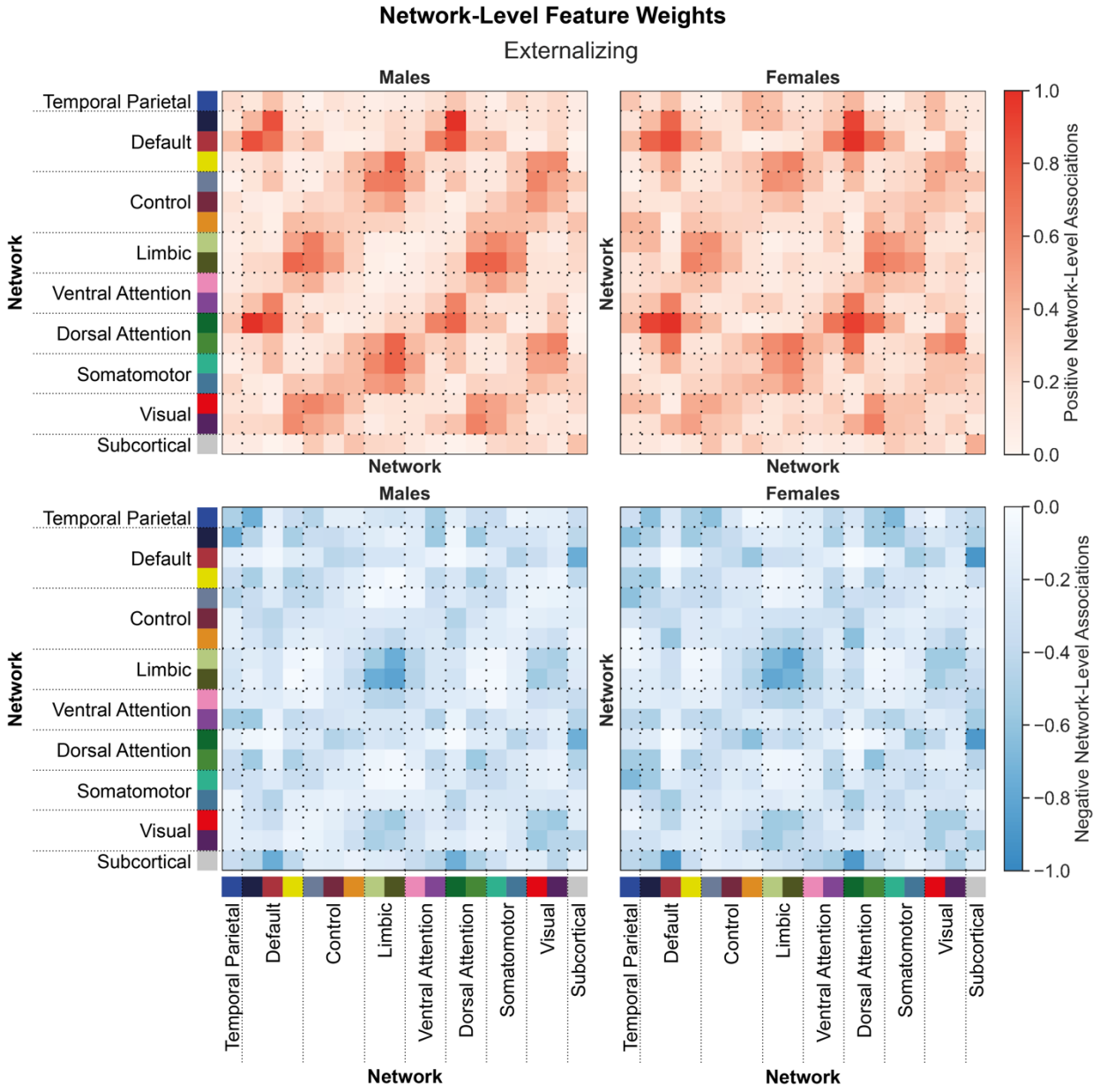

Supplementary Figure 5: Shared network-level functional connections underlying externalizing behaviors in males and females.
Positive (top) and negative (bottom) associations between network-level functional connectivity and externalizing behaviors in males (left) and females (right). Regional feature weights were summarized to a network-level by assigning cortical regions to one of 17 Yeo networks, and subcortical regions to a subcortical network. Colors next to the network labels along the vertical and horizontal axes correspond to the network colors from Figure 1C. Warmer colors within the heatmap indicate a positive association and cooler colors indicate a negative association. For visualization, values within each matrix were divided by the absolute maximum value across the positive and negative matrices for each sex. Correlations between positive associations across sexes, $r_{positive}$=0.87. Correlations between negative associations across sexes, $r_{negative}$=0.89.

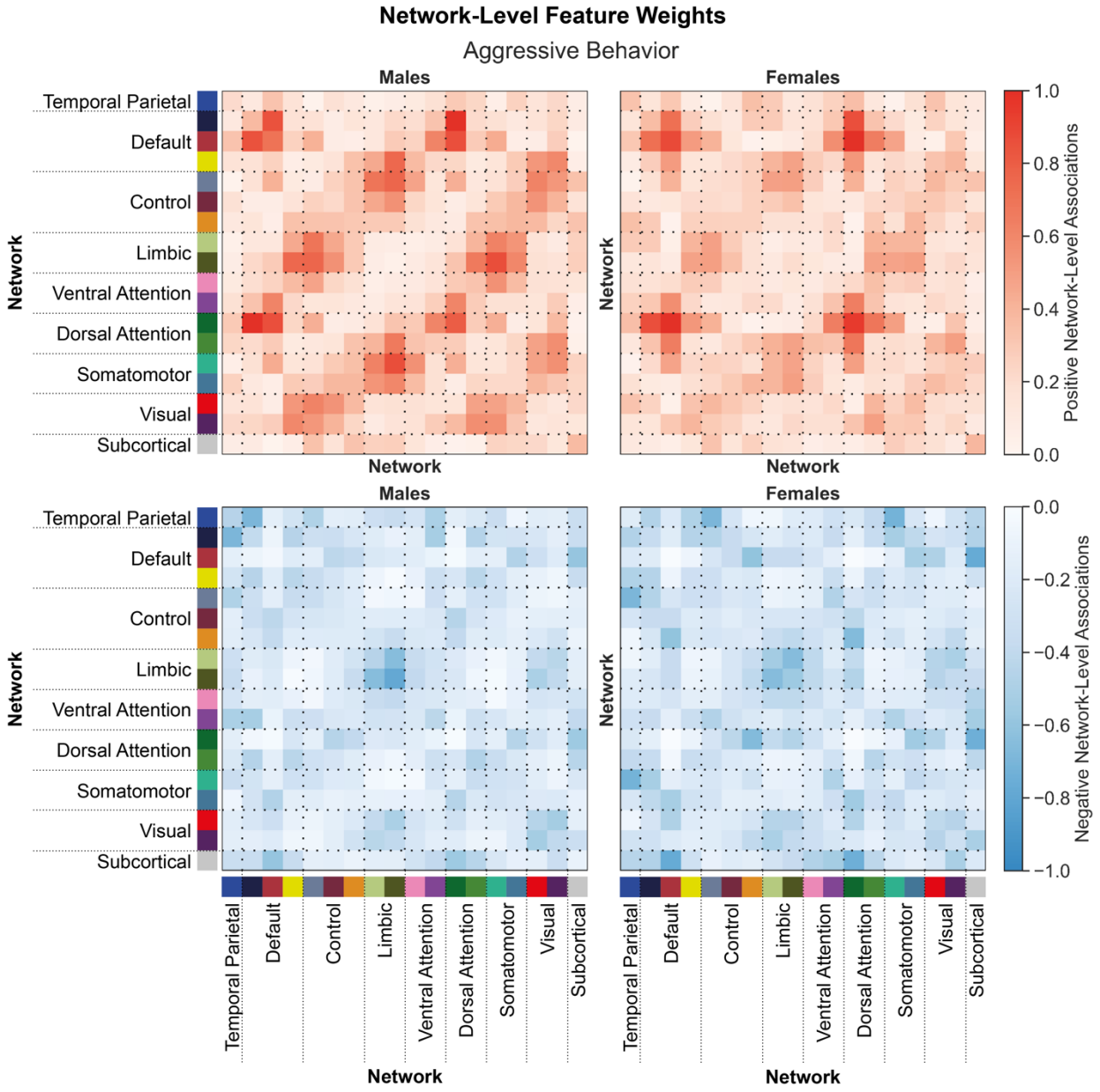

Supplementary Figure 6: Shared network-level functional connections underlying aggressive behaviors in males and females.
Positive (top) and negative (bottom) associations between network-level functional connectivity and aggressive behaviors in males (left) and females (right). Regional feature weights were summarized to a network-level by assigning cortical regions to one of 17 Yeo networks, and subcortical regions to a subcortical network. Colors next to the network labels along the vertical and horizontal axes correspond to the network colors from Figure 1C. Warmer colors within the heatmap indicate a positive association and cooler colors indicate a negative association. For visualization, values within each matrix were divided by the absolute maximum value across the positive and negative matrices for each sex. Correlations between positive associations across sexes, $r_{positive}$=0.80. Correlations between negative associations across sexes, $r_{negative}$=0.75.

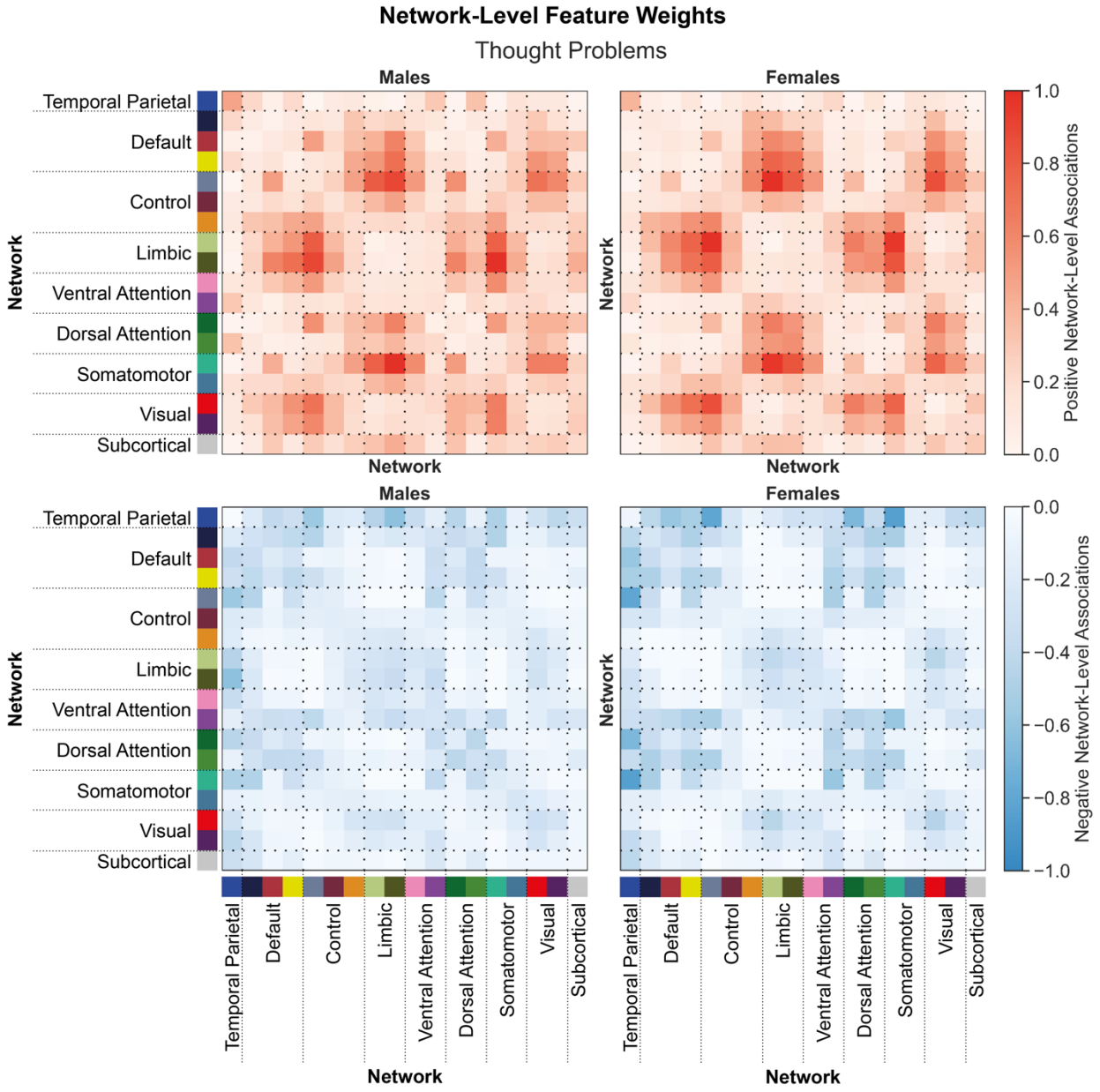

Supplementary Figure 7: Shared network-level functional connections underlying thought problems in males and females.
Positive (top) and negative (bottom) associations between network-level functional connectivity and thought problems in males (left) and females (right). Regional feature weights were summarized to a network-level by assigning cortical regions to one of 17 Yeo networks, and subcortical regions to a subcortical network. Colors next to the network labels along the vertical and horizontal axes correspond to the network colors from Figure 1C. Warmer colors within the heatmap indicate a positive association and cooler colors indicate a negative association. For visualization, values within each matrix were divided by the absolute maximum value across the positive and negative matrices for each sex. Correlations between positive associations across sexes, $r_{positive}$=0.91. Correlations between negative associations across sexes, $r_{negative}$=0.86.

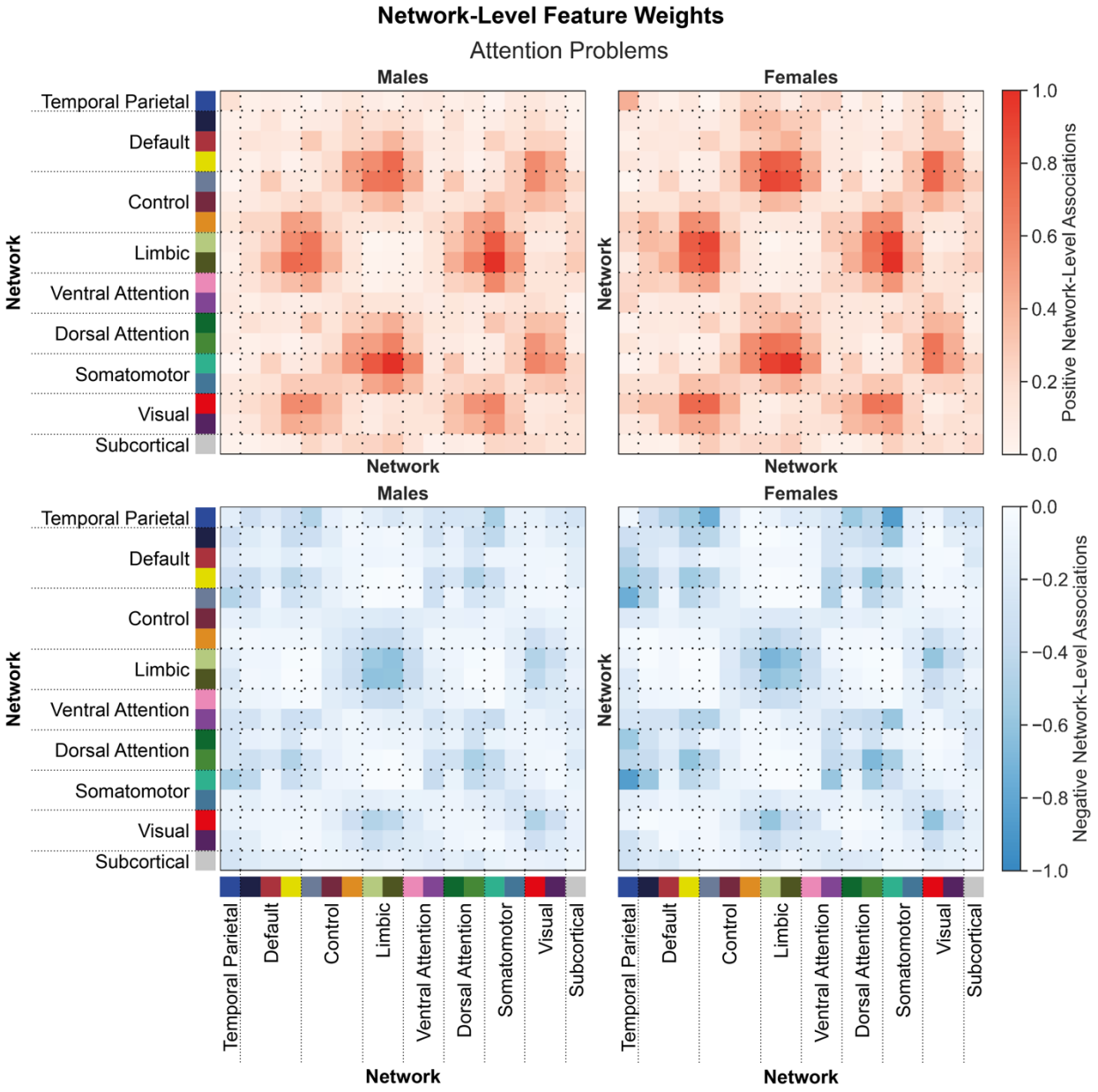

Supplementary Figure 8: Shared network-level functional connections underlie attention problems in males and females.
Positive (top) and negative (bottom) associations between network-level functional connectivity and attention problems in males (left) and females (right). Regional feature weights were summarized to a network-level by assigning cortical regions to one of 17 Yeo networks, and subcortical regions to a subcortical network. Colors next to the network labels along the vertical and horizontal axes correspond to the network colors from Figure 1C. Warmer colors within the heatmap indicate a positive association and cooler colors indicate a negative association. For visualization, values within each matrix were divided by the absolute maximum value across the positive and negative matrices for each sex. Correlations between positive associations across sexes, $r_{positive}$=0.95. Correlations between negative associations across sexes, $r_{negative}$=0.94.

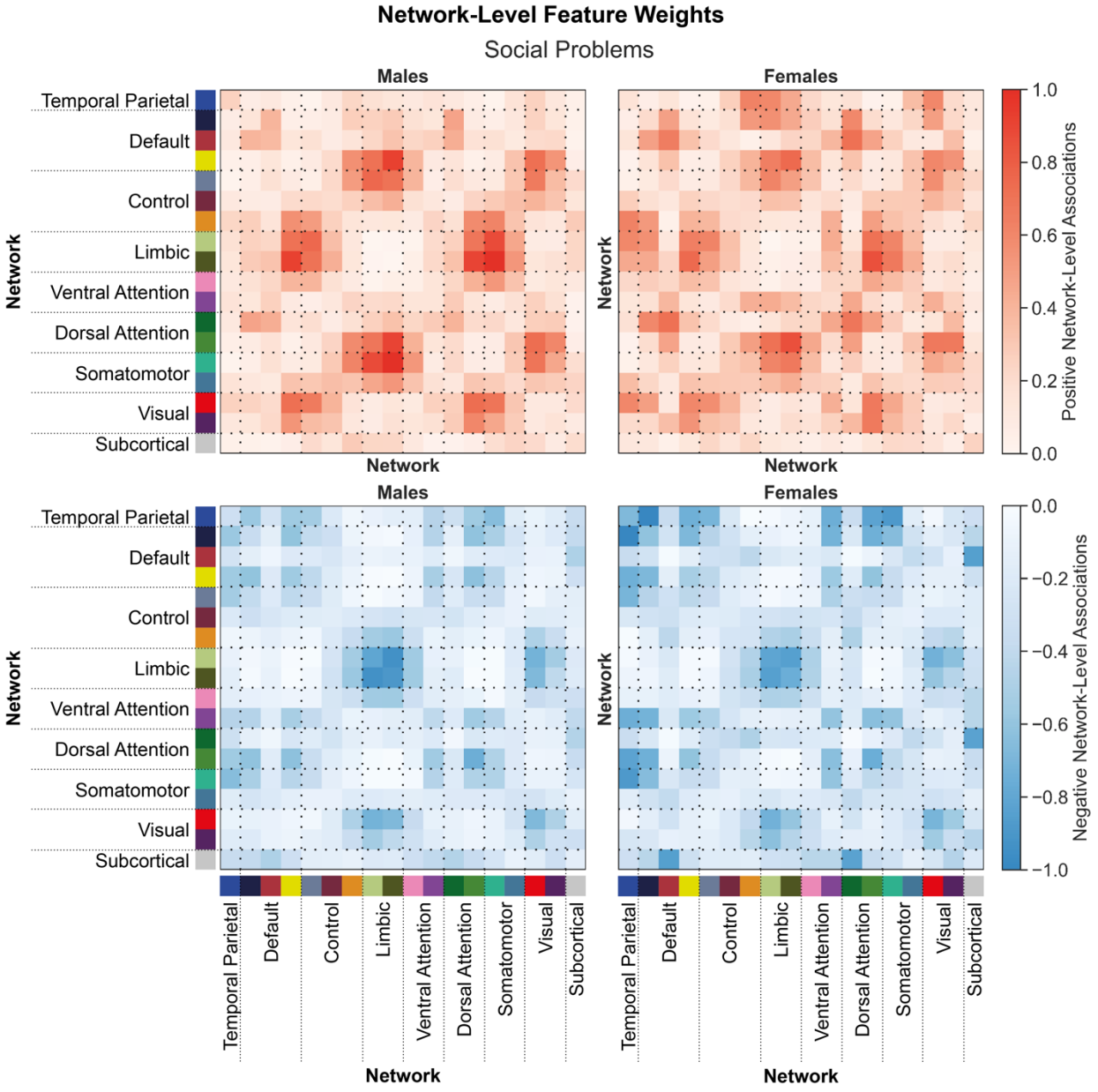

Supplementary Figure 9: Shared network-level functional connections underlying social problems in males and females.
Positive (top) and negative (bottom) associations between network-level functional connectivity and social problems in males (left) and females (right). Regional feature weights were summarized to a network-level by assigning cortical regions to one of 17 Yeo networks, and subcortical regions to a subcortical network. Colors next to the network labels along the vertical and horizontal axes correspond to the network colors from Figure 1C. Warmer colors within the heatmap indicate a positive association and cooler colors indicate a negative association. For visualization, values within each matrix were divided by the absolute maximum value across the positive and negative matrices for each sex. Correlations between positive associations across sexes, $r_{positive}$=0.82. Correlations between negative associations across sexes, $r_{negative}$=0.90.

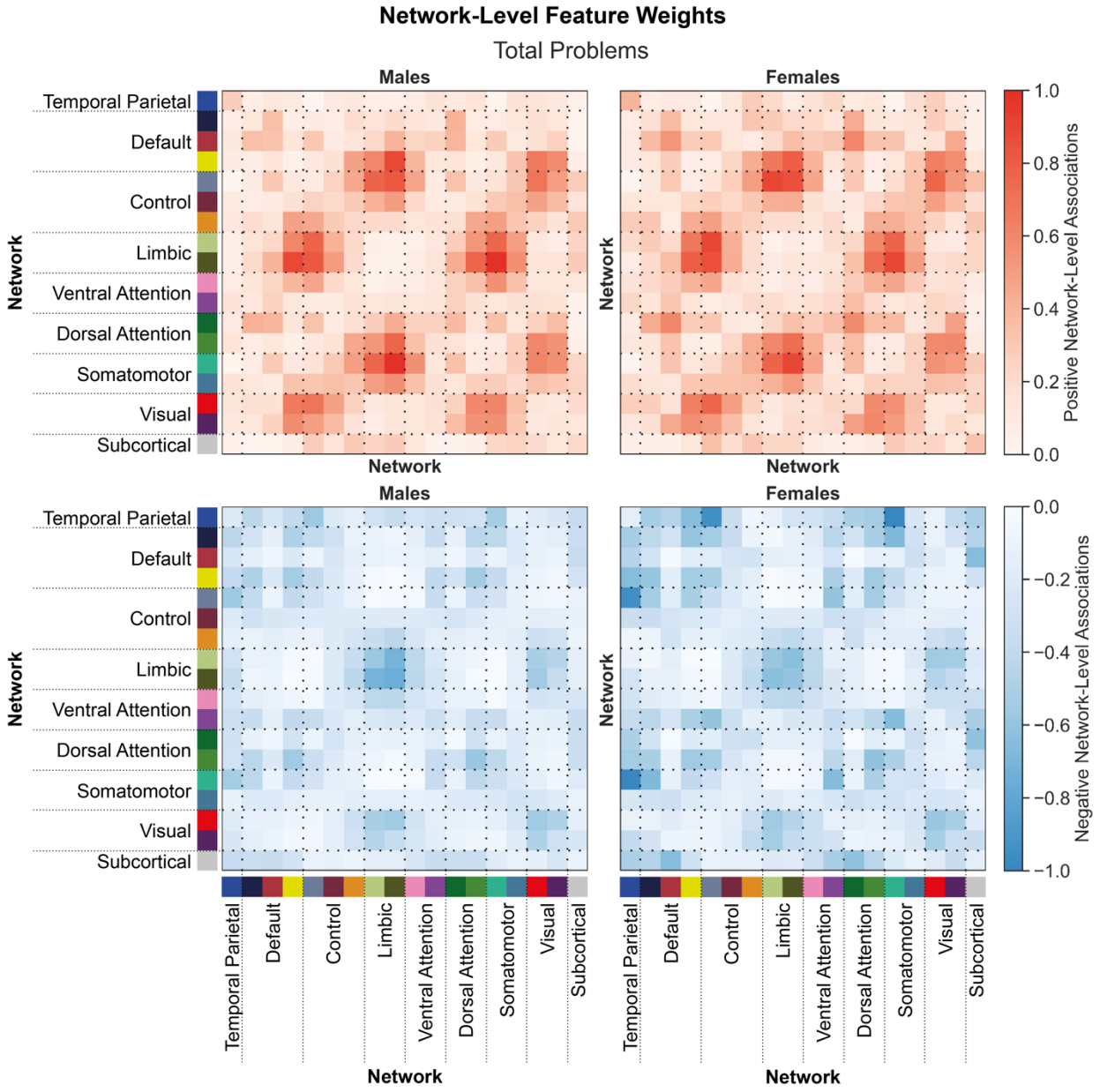

Supplementary Figure 10: Shared network-level functional connections underlying total problems in males and females.
Positive (top) and negative (bottom) associations between network-level functional connectivity and total problems in males (left) and females (right). Regional feature weights were summarized to a network-level by assigning cortical regions to one of 17 Yeo networks, and subcortical regions to a subcortical network. Colors next to the network labels along the vertical and horizontal axes correspond to the network colors from Figure 1C. Warmer colors within the heatmap indicate a positive association and cooler colors indicate a negative association. For visualization, values within each matrix were divided by the absolute maximum value across the positive and negative matrices for each sex. Correlations between positive associations across sexes, $r_{positive}$=0.95. Correlations between negative associations across sexes, $r_{negative}$=0.88.

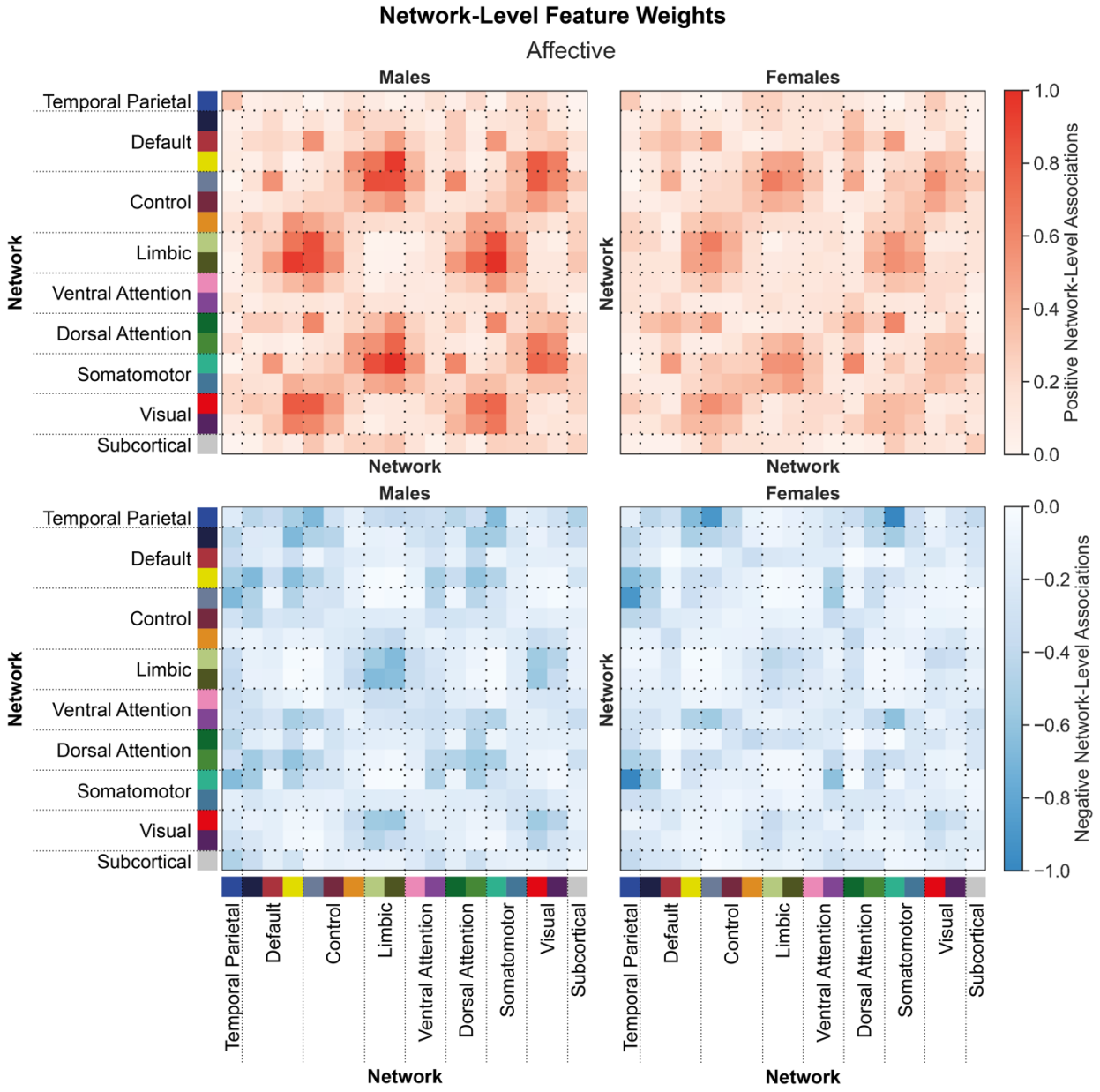

Supplementary Figure 11: Shared network-level functional connections underlying affective scores in males and females.
Positive (top) and negative (bottom) associations between network-level functional connectivity and affective scores in males (left) and females (right). Regional feature weights were summarized to a network-level by assigning cortical regions to one of 17 Yeo networks, and subcortical regions to a subcortical network. Colors next to the network labels along the vertical and horizontal axes correspond to the network colors from Figure 1C. Warmer colors within the heatmap indicate a positive association and cooler colors indicate a negative association. For visualization, values within each matrix were divided by the absolute maximum value across the positive and negative matrices for each sex. Correlations between positive associations across sexes, $r_{positive}$=0.81. Correlations between negative associations across sexes, $r_{negative}$=0.75.

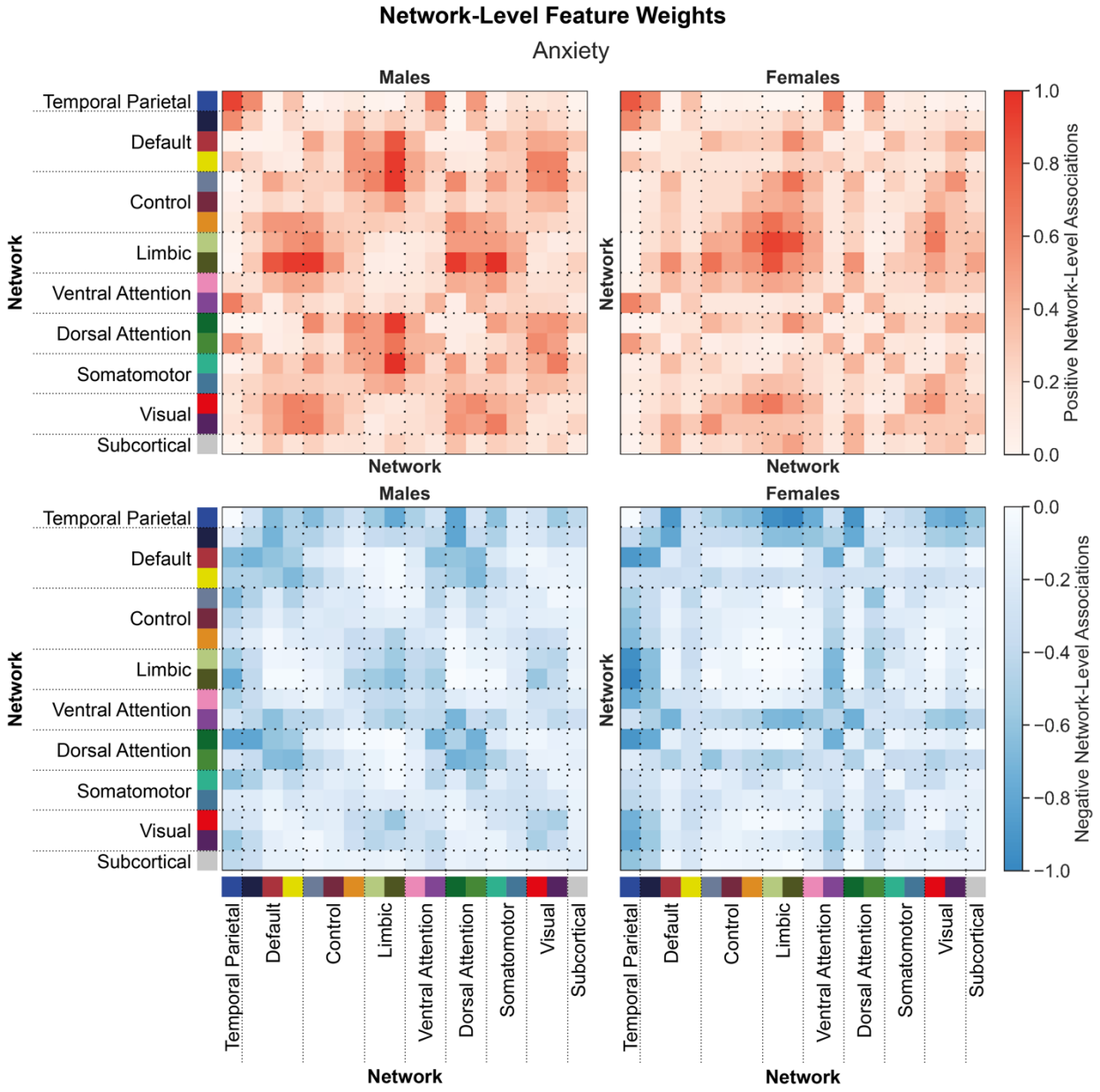

Supplementary Figure 12: Shared network-level functional connections underlying anxiety scores in males and females.
Positive (top) and negative (bottom) associations between network-level functional connectivity and anxiety scores in males (left) and females (right). Regional feature weights were summarized to a network-level by assigning cortical regions to one of 17 Yeo networks, and subcortical regions to a subcortical network. Colors next to the network labels along the vertical and horizontal axes correspond to the network colors from Figure 1C. Warmer colors within the heatmap indicate a positive association and cooler colors indicate a negative association. For visualization, values within each matrix were divided by the absolute maximum value across the positive and negative matrices for each sex. Correlations between positive associations across sexes, $r_{positive}$=0.38. Correlations between negative associations across sexes, $r_{negative}$=0.53.

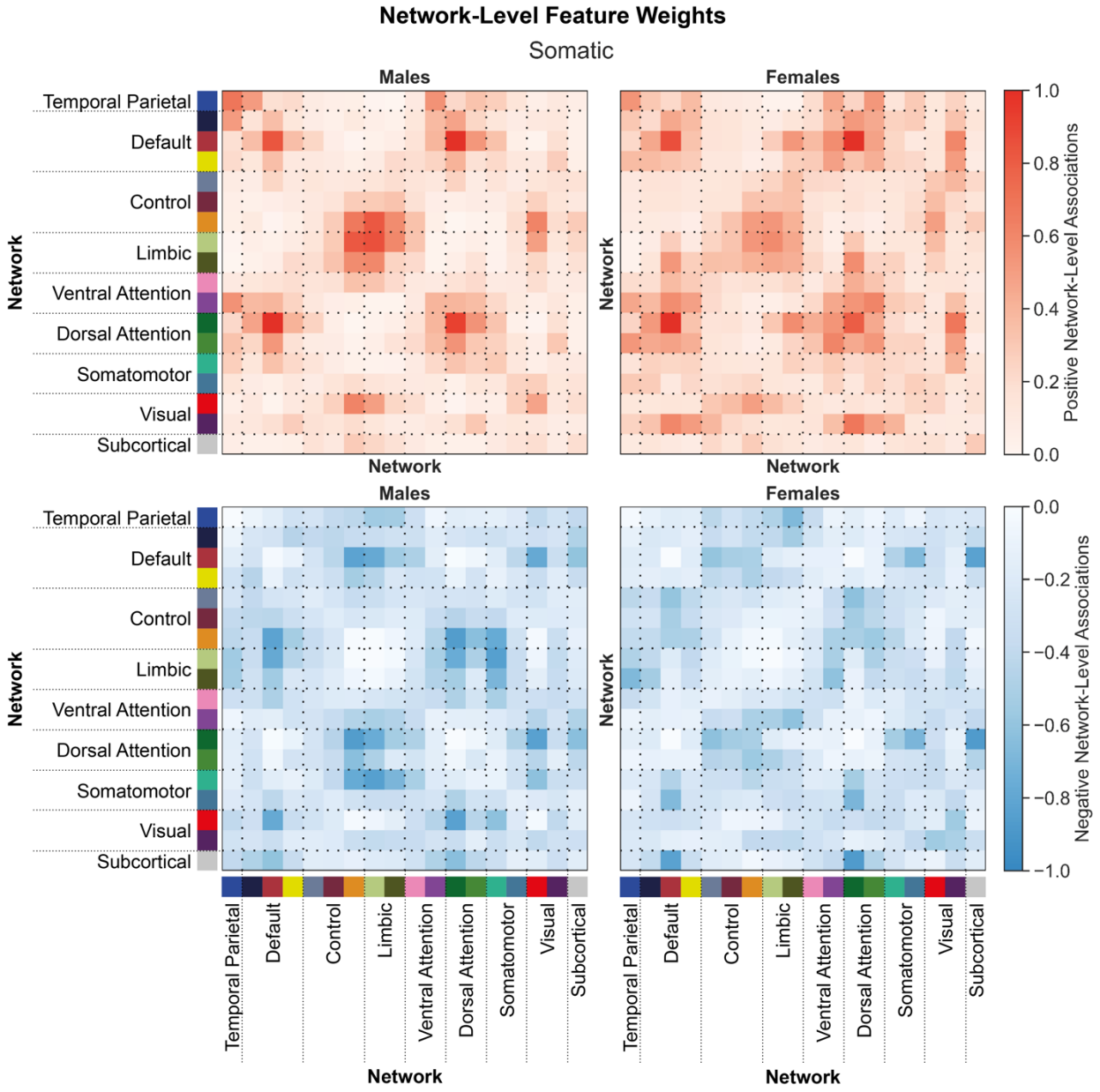

Supplementary Figure 13: Shared network-level functional connections underlying somatic scores in males and females.
Positive (top) and negative (bottom) associations between network-level functional connectivity and somatic scores in males (left) and females (right). Regional feature weights were summarized to a network-level by assigning cortical regions to one of 17 Yeo networks, and subcortical regions to a subcortical network. Colors next to the network labels along the vertical and horizontal axes correspond to the network colors from Figure 1C. Warmer colors within the heatmap indicate a positive association and cooler colors indicate a negative association. For visualization, values within each matrix were divided by the absolute maximum value across the positive and negative matrices for each sex. Correlations between positive associations across sexes, $r_{positive}$=0.76. Correlations between negative associations across sexes, $r_{negative}$=0.56.

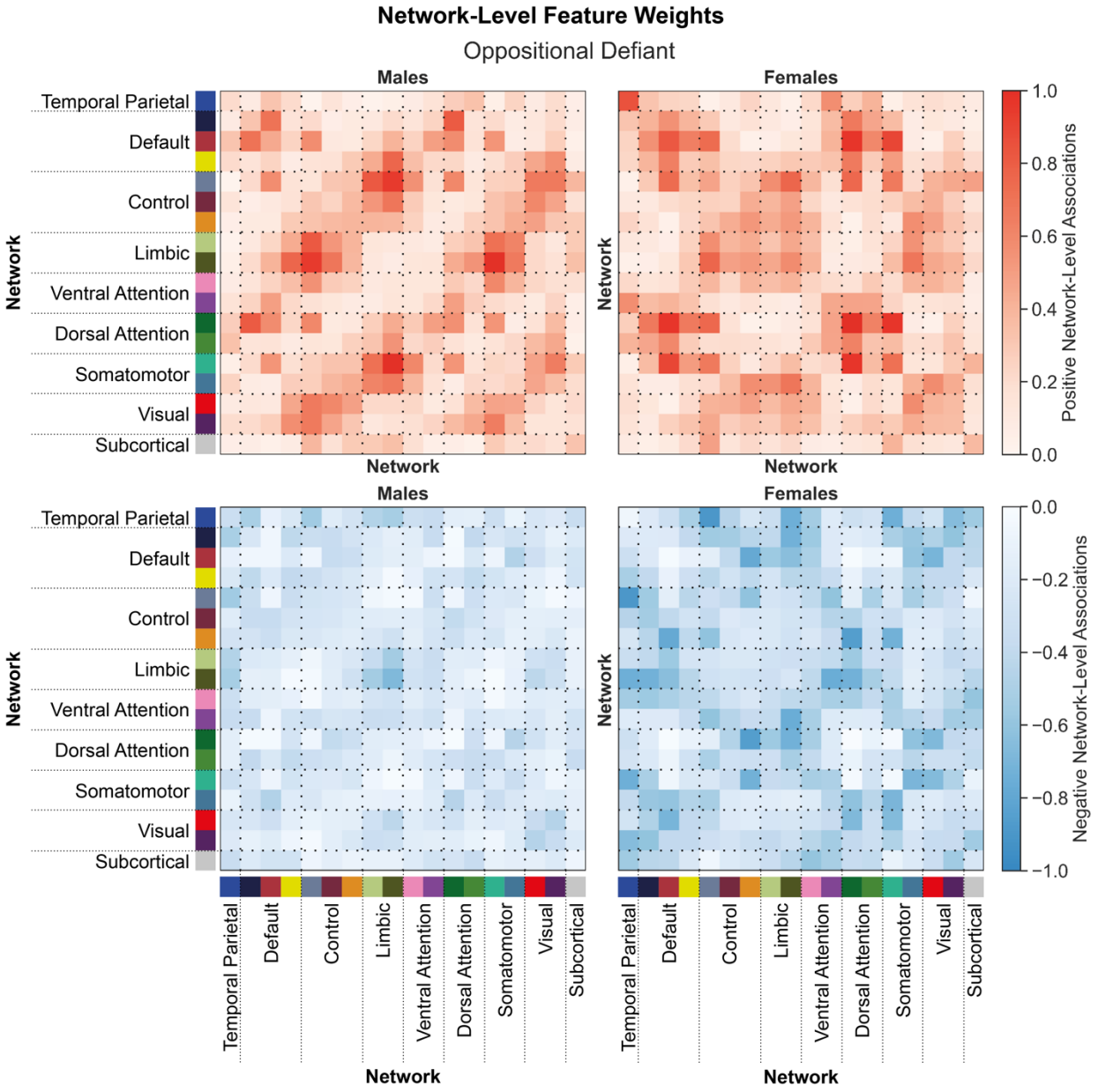

Supplementary Figure 14: Shared network-level functional connections underlying oppositional defiant scores in males and females.
Positive (top) and negative (bottom) associations between network-level functional connectivity and oppositional defiant scores in males (left) and females (right). Regional feature weights were summarized to a network-level by assigning cortical regions to one of 17 Yeo networks, and subcortical regions to a subcortical network. Colors next to the network labels along the vertical and horizontal axes correspond to the network colors from Figure 1C. Warmer colors within the heatmap indicate a positive association and cooler colors indicate a negative association. For visualization, values within each matrix were divided by the absolute maximum value across the positive and negative matrices for each sex. Correlations between positive associations across sexes, $r_{positive}$=0.50. Correlations between negative associations across sexes, $r_{negative}$=0.27.

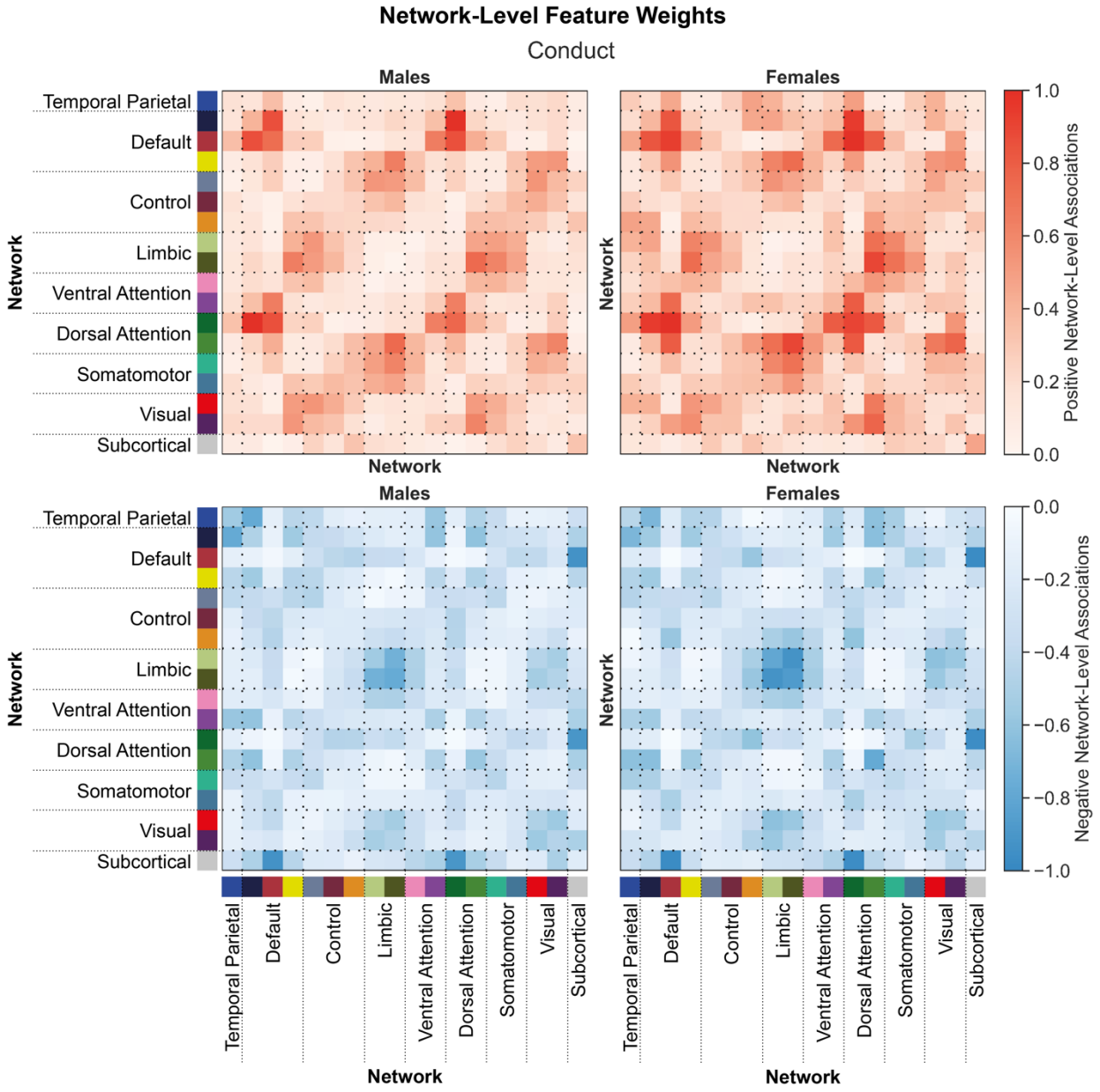

Supplementary Figure 15: Shared network-level functional connections underlying conduct scores in males and females.
Positive (top) and negative (bottom) associations between network-level functional connectivity and conduct scores in males (left) and females (right). Regional feature weights were summarized to a network-level by assigning cortical regions to one of 17 Yeo networks, and subcortical regions to a subcortical network. Colors next to the network labels along the vertical and horizontal axes correspond to the network colors from Figure 1C. Warmer colors within the heatmap indicate a positive association and cooler colors indicate a negative association. For visualization, values within each matrix were divided by the absolute maximum value across the positive and negative matrices for each sex. Correlations between positive associations across sexes, $r_{positive}$=0.89. Correlations between negative associations across sexes, $r_{negative}$=0.93.

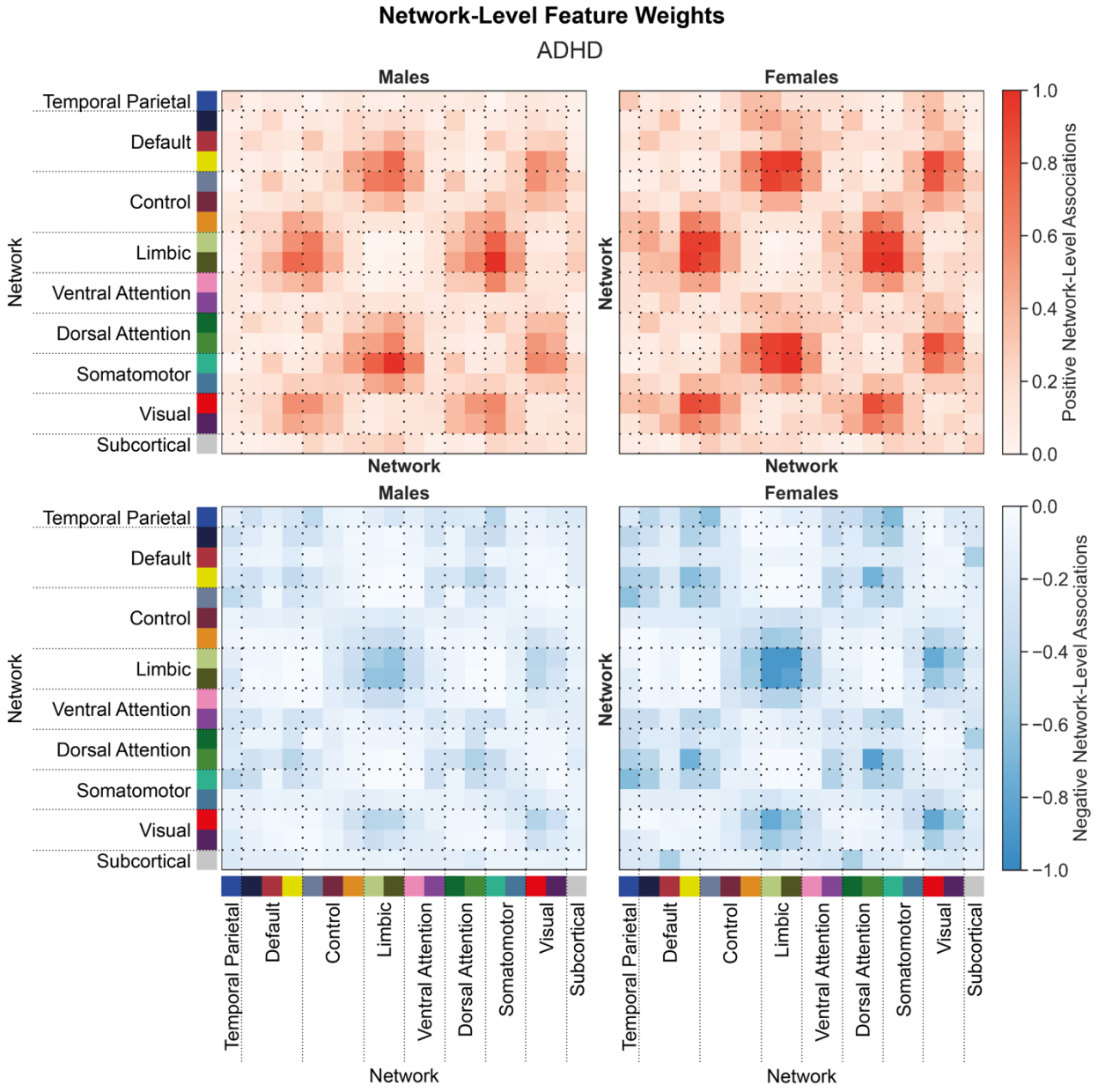

Supplementary Figure 16: Shared network-level functional connections underlying ADHD scores in males and females.
Positive (top) and negative (bottom) associations between network-level functional connectivity and ADHD scores in males (left) and females (right). Regional feature weights were summarized to a network-level by assigning cortical regions to one of 17 Yeo networks, and subcortical regions to a subcortical network. Colors next to the network labels along the vertical and horizontal axes correspond to the network colors from Figure 1C. Warmer colors within the heatmap indicate a positive association and cooler colors indicate a negative association. For visualization, values within each matrix were divided by the absolute maximum value across the positive and negative matrices for each sex. Correlations between positive associations across sexes, $r_{positive}$=0.91. Correlations between negative associations across sexes, $r_{negative}$=0.94.

Supplementary References

1. Ooi LQR, Chen J, Zhang S, Kong R, Li J, Dhamala E, et al. (2022): Comparison of individualized behavioral predictions across anatomical, diffusion and functional connectivity MRI. *BioRxiv*.
2. Chen J, Tam A, Kebets V, Orban C, Ooi LQR, Asplund CL, et al. (2022): Shared and unique brain network features predict cognitive, personality, and mental health scores in the ABCD study. *Nat Commun*. 13:2217.
3. Hagler DJ, Jr., Hatton S, Cornejo MD, Makowski C, Fair DA, Dick AS, et al. (2019): Image processing and analysis methods for the Adolescent Brain Cognitive Development Study. *Neuroimage*. 202:116091.
4. Gordon EM, Laumann TO, Adeyemo B, Huckins JF, Kelley WM, Petersen SE (2016): Generation and evaluation of a cortical area parcellation from resting-state correlations. *Cerebral cortex*. 26:288-303.
5. Kong R, Li J, Orban C, Sabuncu MR, Liu H, Schaefer A, et al. (2018): Spatial Topography of Individual-Specific Cortical Networks Predicts Human Cognition, Personality, and Emotion. *Cerebral Cortex*. 29:2533-2551.
6. Achenbach TM (2001): Manual for ASEBA school-age forms & profiles. *University of Vermont, Research Center for Children, Youth & Families*.
7. Dale AM, Fischl B, Sereno MI (1999): Cortical surface-based analysis. I. Segmentation and surface reconstruction. *Neuroimage*. 9:179-194.
8. Fischl B, Liu A, Dale AM (2001): Automated manifold surgery: constructing geometrically accurate and topologically correct models of the human cerebral cortex. *IEEE Trans Med Imaging*. 20:70-80.
9. Fischl B, Sereno MI, Dale AM (1999): Cortical surface-based analysis. II: Inflation, flattening, and a surface-based coordinate system. *Neuroimage*. 9:195-207.
10. Fischl B, Sereno MI, Tootell RB, Dale AM (1999): High-resolution intersubject averaging and a coordinate system for the cortical surface. *Hum Brain Mapp*. 8:272-284.
11. Greve DN, Fischl B (2009): Accurate and robust brain image alignment using boundary-based registration. *Neuroimage*. 48:63-72.
12. Jenkinson M, Bannister P, Brady M, Smith S (2002): Improved optimization for the robust and accurate linear registration and motion correction of brain images. *Neuroimage*. 17:825-841.
13. Power JD, Barnes KA, Snyder AZ, Schlaggar BL, Petersen SE (2012): Spurious but systematic correlations in functional connectivity MRI networks arise from subject motion. *Neuroimage*. 59:2142-2154.
14. Power JD, Lynch CJ, Silver BM, Dubin MJ, Martin A, Jones RM (2019): Distinctions among real and apparent respiratory motions in human fMRI data. *NeuroImage*. 201:116041.
15. Fair DA, Miranda-Dominguez O, Snyder AZ, Perrone A, Earl EA, Van AN, et al. (2020): Correction of respiratory artifacts in MRI head motion estimates. *Neuroimage*. 208:116400.
16. Gratton C, Dworetsky A, Coalson RS, Adeyemo B, Laumann TO, Wig GS, et al. (2020): Removal of high frequency contamination from motion estimates in single-band fMRI saves data without biasing functional connectivity. *Neuroimage*. 217:116866.
17. Greene AS, Gao S, Scheinost D, Constable RT (2018): Task-induced brain state manipulation improves prediction of individual traits. *Nature communications*. 9:1-13.
18. Li JW, Kong R, Liegeois R, Orban C, Tan YR, Sun NB, et al. (2019): Global signal regression strengthens association between resting-state functional connectivity and behavior. *Neuroimage*. 196:126-141.
19. Power JD, Mitra A, Laumann TO, Snyder AZ, Schlaggar BL, Petersen SE (2014): Methods to detect, characterize, and remove motion artifact in resting state fMRI. *Neuroimage*. 84:320-341.

20. Benjamini Y, Hochberg Y (1995): Controlling the False Discovery Rate - a Practical and Powerful Approach to Multiple Testing. *J R Stat Soc B*. 57:289-300.
21. Haufe S, Meinecke F, Görgen K, Dähne S, Haynes J-D, Blankertz B, et al. (2014): On the interpretation of weight vectors of linear models in multivariate neuroimaging. *Neuroimage*. 87:96-110.
22. Tian Y, Zalesky A (2021): Machine learning prediction of cognition from functional connectivity: Are feature weights reliable? *bioRxiv*.
23. Chen J, Ooi LQR, Li J, Asplund CL, Eickhoff SB, Bzdok D, et al. (2022): There is no fundamental trade-off between prediction accuracy and feature importance reliability. *bioRxiv*.
24. Dhamala E, Jamison KW, Jaywant A, Kuceyeski A (2022): Shared functional connections within and between cortical networks predict cognitive abilities in adult males and females. *Hum Brain Mapp*.
25. Yeo BT, Krienen FM, Sepulcre J, Sabuncu MR, Lashkari D, Hollinshead M, et al. (2011): The organization of the human cerebral cortex estimated by intrinsic functional connectivity. *Journal of neurophysiology*. 106:1125-1165.